Global Change Biology

Global Change Biology (2010) **16**, 605–616, doi: 10.1111/j.1365-2486.2009.02033.x

Changes in the abundance of C3/C4 species of Inner Mongolia grassland: evidence from isotopic composition of soil and vegetation

MAXIMILIAN H. O. M. WITTMER*, KARL AUERSWALD*, YONGFEI BAI†, RUDI SCHÄUFELE* and HANS SCHNYDER*

*Lehrstuhl für Grünlandlehre, Technische Universität München, Am Hochanger 1, D-85350 Freising-Weihenstephan, Germany, †State Key Laboratory of Vegetation and Environmental Change, Institute of Botany, Chinese Academy of Sciences, 20 Nanxincun, Xiangshan, Beijing 100093, China

Abstract

Global warming, increasing CO_2 concentration, and environmental disturbances affect grassland communities throughout the world. Here, we report on variations in the C3/C4 pattern of Inner Mongolian grassland derived from soil and vegetation. Soil samples from 149 sites covering an area of approximately 250 000 km^2 within Inner Mongolia, People's Republic of China were analyzed for the isotopic composition (δ^{13}C) of soil organic carbon (SOC). The contrast in δ^{13}C between C3 and C4 plants allowed for calculation of the C3/C4 ratio from δ^{13}C of SOC with a two-member mixing model, which accounted for influences of aridity and altitude on δ^{13}C of the C3 end-member and for changes in δ^{13}C of atmospheric CO_2. Maps were created geostatistically, and showed a substantially lower C4 abundance in soil than in recent vegetation (−10%). The difference between soil and vegetation varied regionally and was most pronounced within an E–W belt along 44°N and in a mountainous area, suggesting a spread of C4 plants toward northern latitudes (about 1°) and higher altitudes. The areas of high C4 abundance for present vegetation and SOC were well delineated by the isotherms of crossover temperature based on the climatic conditions of the respective time periods. Our study indicates that change in the patterns of C3/C4 composition in the Inner Mongolia grassland was mainly triggered by increasing temperature, which overrode the antagonistic effect of rising CO_2 concentrations.

Keywords: δ^{13}C, carbon isotope discrimination, crossover temperature, geostatistics, precipitation, semivariogram, soil organic carbon, Suess effect, wool

Received 29 January 2009; revised version received 18 May 2009 and accepted 9 July 2009

Introduction

The carbon isotope composition (δ^{13}C) of plants and soil organic carbon (SOC) yields important information regarding carbon fluxes and linked biogeochemical cycles (Schimel, 1995; Ehleringer *et al*., 2000). In grassland, the ^{13}C signal can vary considerably. This is related primarily to the presence of variable proportions of C3 and C4 photosynthetic types (Bird & Pousai, 1997; Tieszen *et al*., 1997; Collatz *et al*., 1998) and the large difference in carbon isotope discrimination ($^{13}\Delta$) between them (Farquhar *et al*., 1989). Variation in the C3/C4 ratio has wide biogeochemical and land use implications: it affects the magnitude and seasonal distribution of biomass production, soil carbon storage, water use, and nutrient cycling (Bird & Pousai, 1997; Tieszen *et al*., 1997; Epstein *et al*., 1998; Sage & Kubien, 2003; Semmartin *et al*., 2004). Hence, because it indicates the C3/C4 ratio, δ^{13}C is a useful proxy of vital functions of grassland. However, only a few regional-scale investigations of δ^{13}C of C3/C4 mixed grassland have been undertaken (von Fischer *et al*., 2008).

Soil is one of the most important terrestrial carbon reservoirs, storing more than twice as much carbon as the atmosphere (Trumbore, 2000). The SOC input to this pool is mainly composed of carbon from vegetation, and the output of carbon is by soil respiration (Schimel, 1995). With increasing soil depth, the soil carbon age increases greatly (e.g. as derived from radiocarbon dating) (Rumpel *et al*., 2002; Dümig *et al*., 2008; Lopez-Capel *et al*., 2008). Hence, SOC is affected by past vegetation, and therefore allows for the reconstruction of changes in the isotopically distinct C3/C4 ratio (Boutton *et al*., 1998; Ehleringer *et al*.,

Correspondence: Karl Auerswald, tel. + 49 8161 713965, fax + 49 8161 713243, e-mail: auerswald@wzw.tum.de

2000; Krull *et al.*, 2005, 2007; von Fischer *et al.*, 2008), while current vegetation is strongly influenced by current environmental conditions.

Modeling has revealed that the Chinese grassland is among the most sensitive ecosystems with regard to climatic changes (Xiao *et al.*, 1995; Gao *et al.*, 2000). This grassland has experienced extensive changes in land use and environmental conditions during the past 50 years: (1) Land use changed from nomadic to sedentary grazing in the 1960s; this change was accelerated following the stimulation of the Chinese economy in the 1990s. (2) The area experienced a temperature increase of approximately 2 °C during the growing period (NOAA NCDC Climate Data Online, 2008), which is one of the largest increases on earth (Yu *et al.*, 2003). (3) Over the last century, the volumetric CO_2 concentration increased by more than 50 ppm.

There is abundant evidence that the current distribution of C4 plants is primarily controlled by growing season temperature (Ehleringer *et al.*, 1997; Collatz *et al.*, 1998) and that this is related to the higher effective quantum yield of CO_2 fixation (Ehleringer & Björkman, 1977) and a higher maximum photosynthetic rate of C4 plants at high temperatures (Sage & Kubien, 2003). C4 dicots predominate in hot, arid, saline, or highly disturbed habitats (Ehleringer *et al.*, 1997). Hence, increasing temperature and land use/disturbance should promote the growth of C4 plants. On the other hand, rising atmospheric CO_2 should favor C3 plants (Collatz *et al.*, 1998). Furthermore, the different influences act on different scales. Land use can vary over a few square kilometers, while temperature varies regionally and CO_2 concentration changes globally. Moreover, the seasonal distribution of precipitation and aridity may exert secondary, modifying effects. For example, a predominance of summer rainfalls typically benefits C4 plants more than C3 plants (Hattersley, 1983; Paruelo & Lauenroth, 1996). Presumably, such secondary controls have their strongest effect on C3/C4 abundance in those regions that have a growing season mean temperature that is near the C3/C4 crossover temperature (i.e. the temperature above which the light use efficiency of C4 plants is higher than that of C3 plants; see Ehleringer *et al.*, 1997; Still *et al.*, 2003). In this respect, the grassland of Inner Mongolia is of particular interest, because the average temperature during the summer months is close to the crossover temperature when most of the annual precipitation falls (especially July). There are several reports indicating increases in the number and abundance of C4 species with increasing aridity in (Inner) Mongolia grassland (Pyankov *et al.*, 2000; Wang, 2004) and desertification (Wang, 2002), although conflicting evidence has also been presented (Ni, 2003; Wang, 2003). However, a quantitative, regionalized assessment in terms of biomass is absent.

The spatial variation of C3/C4 species contributing to biomass was determined for recent vegetation by Auerswald *et al.* (2009), who made use of the 'sampling' activity of livestock. By grazing the grassland, livestock integrate the carbon isotope information of the grazed vegetation over the entire growing period and the entire grazed area depositing isotopic information from present-day vegetation in wool growth. The soil carbon pool, due to its slow turnover, should contain information of former vegetation. Hence, the aim of this work was to compare the isotopic records of soil and vegetation in a large area of Inner Mongolia using geostatistical tools. Specifically, we address the following questions: (1) Which C3/C4 pattern is reflected by the $\delta^{13}C$ of SOC? (2) How do present-day vegetation patterns match with those of SOC? (3) Are differences between former and present-day C3/C4 patterns related to environmental patterns?

Materials and methods

Study area

The study area was situated between 111°38′ and 117°49′E (approximately 500 km) and 41°30′ and 45°46′N (approximately 450 km) in the Inner Mongolia Autonomous Region in the Peoples Republic of China (Fig. 1). Sampled altitudes ranged from 800 to 1700 m above sea level (a.s.l.). Mean annual precipitation (MAP) increases from 100 mm yr^{-1} in the western region near the Gobi desert to 400 mm yr^{-1} in the eastern region. Most of the precipitation (approximately 75%) falls during the growing period (April–September). Mean annual temperature (MAT) and mean temperature of the growing period vary from 0 to 6 °C and 14 to 19 °C, respectively. The soils in the eastern region are mostly Haplic Kastanozems and Chernozems on loesslike substrates, whereas Calcisols and Cambisols are more common in the western region (Li *et al.*, 1978). Almost the entire area is used for small ruminant livestock production (mainly sheep and cashmere goats) with little agriculture, which consists mainly of vegetables and other crops to supplement the human diet, and some maize.

Sampling, sample preparation, and analysis

The steps from sampling the soil to the interpolated maps, which are necessary to derive C3/C4 pattern from soils, are illustrated as a flow chart in Fig. 2. Samples were collected in August/September 2003, August/September 2004, and June/July 2007. The sampling area (106°12′–118°54′E and 40°36′–46°37′N) exceeded the study area to avoid boundary effects at the periphery of the study area during spatial analysis and interpolation. Sampling positions and altitudes were measured

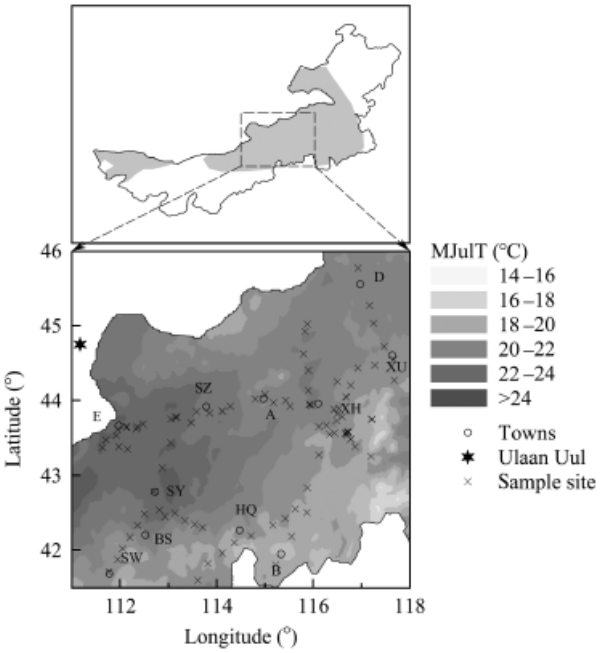

Fig. 1 *Top:* Study area (rectangle) within the grassland (shaded area) of Inner Mongolia, P.R. China (contour). *Bottom:* Mean July temperature (MJulT, normal period 1961–90) and sampling sites. The star denotes the NOAA/CMDL station in Ulaan Uul. Towns are A, Abag Qi; B, Baochang; BS, Bayan Sum; D, Dong Ujimqin Qi; E, Erenhot; HQ, Huang Qi; SW, Siziwang; SY, Sonid Youqi; SZ, Sonid Zuoqi; XH, Xilinhot; XU, Xi Ujimqin Qi.

with a mobile GPS. Soil was sampled to a depth of approximately 10 cm within an area of approximately $20 \times 20\,cm^2$. Altogether 149 samples were taken, ten of them were beyond the periphery of the study area to enhance the spatial interpolation and reduce the error at the boundaries.

Stones, roots, and litter were removed; the soil was sieved (1 mm), and subsamples were ground to homogeneity with a ball mill after being dried for 48 h at 40 °C. Samples were weighed into silver cups and moistened with 15 μL of de-ionized water. Carbonates were then removed by acid fumigation above a 12 N HCl solution for 24 h (modified after Harris *et al*., 2001). Afterwards samples were dried at 60 °C for 12 h. Depending on SOC content, 7–15 mg of soil in silver cups coated with tin cups were analyzed for their isotopic composition.

The carbon isotope composition was determined with an elemental analyzer (NA 1110; Carlo Erba, Milan, Italy) interfaced (ConFlo III; Finnigan MAT, Bremen, Germany) to an isotope ratio mass spectrometer (Delta Plus; Finnigan MAT). Carbon isotopic data are presented as $\delta^{13}C$, with $\delta^{13}C = (R_{sample}/R_{standard})-1$, where R is the $^{13}C/^{12}C$ ratio and standard is the Vienna Pee Dee Belemnite standard. Each sample was measured against a laboratory working standard CO_2 gas, which was previously calibrated against an IAEA secondary standard (IAEA-CH6, accuracy of calibration 0.06‰ SD). After every tenth sample a solid internal lab standard (SILS) with similar C/N ratio as the sample material (fine ground wheat flour for plant samples; protein powder for wool) was run as a blind control. The SILS were previously calibrated against an international standard (IAEA-CH6). The precision for sample repeats was 0.22‰ (SD).

Carbon isotope discrimination of plants and retrieval from SOC

The $\delta^{13}C$ of plants ($\delta^{13}C_p$) differs from the $\delta^{13}C$ of air ($\delta^{13}C_a$) depending on the discrimination $^{13}\Delta_p$ (Farquhar *et al*., 1989):

$$^{13}\Delta_p = \frac{\delta^{13}C_a - \delta^{13}C_p}{1 + \delta^{13}C_p}, \quad (1)$$

with $\delta^{13}C_a$ continuously decreasing over time as a consequence of the CO_2 accumulation in the atmosphere (i.e. Suess-effect). Assuming that SOC originates entirely from plant material, $^{13}\Delta_p$ can be calculated from the $\delta^{13}C$ of SOC ($\delta^{13}C_{SOC}$). However, an isotopic shift between plant and soil carbon must be considered. This varies with soil depth and, hence, integration time, and is termed inherent fractionation (Krull *et al*., 2005). The inherent fractionation can be attributed to several processes, such as preferential degradation of some plant materials, microbiological and invertebrate activity, Suess effect, and adsorption processes (see discussions by Ehleringer *et al*., 2000; Santruckova *et al*., 2000; Krull *et al*., 2005). The inherent fractionation usually ranges between 1‰ and 3‰ enrichment (Krull *et al*., 2005). However, it is difficult to find a fixed value for the fractionation from paired samples of soil and plant material due to the large difference in integration time between both pools and the multitude of influences, which may differ in importance between sites. This is especially true when a change in the C3/C4 ratio affects the pools. In mixed C3/C4 grassland, the $\delta^{13}C_{SOC}$ of the A horizon is enriched by approximately 1‰ compared with the present standing biomass (Krull *et al*., 2005; von Fischer *et al*., 2008). Because we only sampled the A horizon and we explicitly accounted for the Suess effect, which corresponds to approximately 1.2‰ (see Supporting Information), we assumed no further inherent fractionation. Yet, we discuss related phenomena.

Atmospheric isotope composition, CO_2 concentration, and crossover temperature

When determining the C3/C4 vegetation pattern from SOC, one must address the fact that SOC comprises

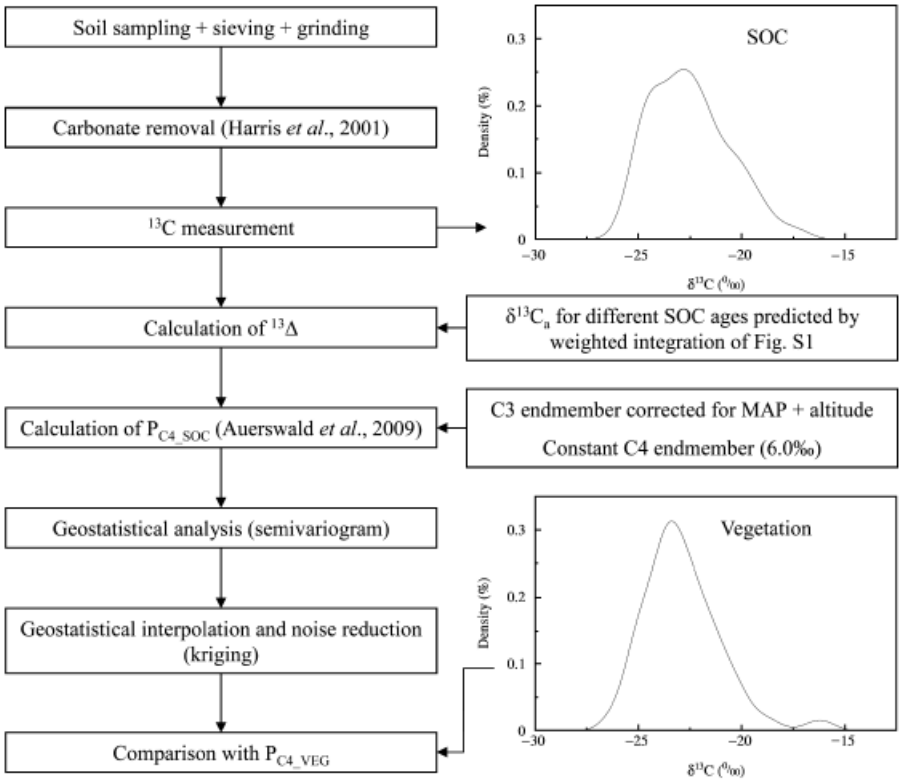

Fig. 2 Flow chart of the individual steps from sampling the soil to the P_{C4} map. Graphs present the density estimation of $\delta^{13}C$ of SOC (top) and $\delta^{13}C$ of vegetation (bottom).

plant material in varying proportions from different years. As $\delta^{13}C_a$ changes over time (Suess effect) so does the respective $\delta^{13}C_p$ (Zhao *et al.*, 2001). Hence, one must know how $\delta^{13}C_a$ has changed, and during approximately which years the SOC originated. $\delta^{13}C_a$ and CO_2 concentrations are known from ice-core studies (Friedli *et al.*, 1986; Francey *et al.*, 1999) and from atmospheric monitoring (Keeling *et al.*, 1979; Friedli *et al.*, 1986; Conway *et al.*, 1994; Francey *et al.*, 1999; Gat *et al.*, 2001; Allison *et al.*, 2003; NOAA ESRL, 2008; $n = 62$). Because the changes do not follow a general trend, three time periods with overlapping cubic functions were fitted to the $\delta^{13}C_a$ data (see Supporting Information), yielding a continuous estimate of mean annual values for each year back to 1700. The root mean squared error (RMSE) for the predicted $\delta^{13}C_a$ was 0.08‰. Further we accounted for a 0.14‰ less negative $\delta^{13}C_a$ during the growing period compared with the annual mean (Wittmer *et al.*, 2008), as derived from air samples at Ulan Uul, a long-term monitoring station in the Republic of Mongolia <50 km northwest of the study area (Tans & Conway, 2005) (Fig. 1).

Because SOC cannot be assigned to a particular year, we accounted for the overall integration by assuming an exponential decay function (Wynn & Bird, 2007):

$$D = \exp(-kt_{SOC}), \quad (2)$$

with D denoting the fraction contribution of a certain year t_{soc} (year before present, BP) to SOC. We assumed a maximum SOC age of 700 years and (numerically) varied the decay constant k between 0.02 and 0.003 to obtain mean SOC ages between 50 and 300 years. For example, a decay constant of 0.02 corresponded to a 'fast' decay and thus a relatively recent mean SOC age of 50 years. A weighted mean $\delta^{13}C_a$ was then calculated based on the respective decay function. For further calculations we assumed a mean SOC age of 100 years, and we discuss the implications of different SOC ages (Table 1).

The crossover temperature for quantum yield of CO_2 uptake is a proxy for the physiological mechanisms explaining the C3/C4 distribution along temperature and CO_2 concentration gradients according to Collatz *et al.* (1998) (see Eqns (1) and (A1) to (A4) in Collatz *et al.*, 1998). This procedure also accounts for effects of CO_2 concentration on quantum yield. As the latter increased over time, the crossover temperature also increased (see supporting information).

Table 1 Influence of mean SOC age BP on decay-weighted mean volumetric CO_2 concentration in the atmosphere, crossover temperature (i.e. the temperature above which the quantum yield of C4 plants is higher than that of C3 plants), $\delta^{13}C_a$ during the growing period, and the corresponding C4 abundance calculated from SOC when applying the modeled $\delta^{13}C_a$ and averaged over all sampling sites

Mean SOC age (yr)	Volumetric CO_2 concentration (ppm)	Range for crossover temperature (°C)	Decay-weighted $\delta^{13}C_a$ (‰)	Site-mean P_{C4} (%)
50	321	16.3–21.5	−7.23	12.9
75	306	15.5–20.6	−7.04	11.1
100	298	15.0–20.2	−6.88	9.7
150	290	14.6–19.7	−6.78	8.8
200	286	14.3–19.4	−6.67	7.9
300	276	13.7–18.8	−6.52	6.5

The weighted means take into account the change of a variable over time at varying proportions depending on mean SOC age and a first-order decay function [Eqn (2)].

Meteorological data

The long-term averages of the last normal period (1961–1990) of precipitation and temperature (monthly and annual means) were taken from high-resolution maps obtained from The Climate Source LLC, Corvallis, OR, USA (2002). These maps have a pixel resolution of $0.02^\circ \times 0.02^\circ$ (approximately $1.5 \times 1.5\,km^2$), which was judged sufficient to locate the sampling sites. The maps were created using the PRISM method (parameter-elevation regressions on independent slopes model; Daly *et al*., 2002).

Estimation of C4 fraction from SOC and present vegetation

At each site, the C4 fraction (P_{C4}) from SOC (P_{C4_SOC}) was estimated from the $^{13}\Delta_{SOC}$ using a two-member mixing model:

$$P_{C4\_SOC} = \frac{^{13}\Delta_{SOC} - ^{13}\Delta_3}{^{13}\Delta_4 - ^{13}\Delta_3}, \quad (3)$$

where $^{13}\Delta_3$ and $^{13}\Delta_4$ denote the end-members of the mixing model (local $^{13}\Delta$ of pure C3 and C4 vegetation communities, respectively). $^{13}\Delta_4$ was taken as 6.0‰ (Auerswald *et al*., 2009). Regionalized estimates of $^{13}\Delta_3$ were obtained following Auerswald *et al*. (2009):

$$^{13}\Delta_3 = 14.4‰ + 1.1‰\frac{A - 1000}{1000} + 2.7‰\sqrt{P_G}, \quad (4)$$

accounting for precipitation during the growing period (P_G; Wittmer *et al*., 2008) and for altitude (A; Männel *et al*., 2007). P_{C4} for present vegetation (P_{C4_VEG}) covering the period 1998–2007 was taken from Auerswald *et al*. (2009). The latter was estimated from δ^{13}C of woolen samples obtained from sheep grazing within the study area. This approach is advantegeous, as sheep wool integrates over the entire growing period and the grazing area. To obtain δ^{13}C of the vegetation (Fig. 2), a tissue specific discrimination in δ^{13}C between wool and vegetation was taken into account. This approach was discussed and justified in detail by Auerswald *et al*. (2009).

Statistical methods and geostatistical analysis

Linear and multiple regressions were used to evaluate the datasets. The coefficient of determination was tested with a two-sided test for significance of the regression. Hypothesis testing on equal means of groups were carried out using Student's *t*-test. Significance thresholds of $P < 0.05$, < 0.01, and < 0.001 were used. Statistical spread is denoted as SD, standard error (SE), or 95% confidence interval (CI). Kernel densities (Silvermann, 1986) were calculated using Gaussian kernels to yield estimates of the density distribution. Bandwidth of density estimation of different sized data sets was defined *via* Silverman's 'rule of thumb'. To allow for comparison of differently sized data sets integral density was adjusted to unity. All of these procedures followed standard protocols (Sachs & Hedderich, 2006), and were carried out using GNU R 2.7.2 (R Development Core Team, 2008).

Geostatistical analyses (see Rossi *et al*., 1992 and citations therein) were conducted with the auxiliary packages geoR (Ribeiro & Diggle, 2001), gstat (Pebesma, 2004), and PBSmapping (Schnute *et al*., 2008). The semivariance (γ) equals the variance for values at points, which are separated by a certain distance called lag (Bachmaier & Backes, 2008). The semivariances for classes of different lags yielded the empirical semivariogram (*x*-axis: mean lag, *y*-axis: mean semivariance). A theoretical semivariogram was fitted to minimize weighted least squares, with weights calculated from the ratio of pairs within a class to mean lag (Wittmer *et al*., 2008). The theoretical semivariogram delivers three parameters: the nugget effect, the sill, and the range. The nugget effect quantifies the small-scale variation including data uncertainty. The sill quantifies the total variation caused by the nugget effect and the variation due to a spatial pattern. The nugget/sill ratio hence reflects the ratio of random (unexplained by a pattern)-to-total variation. The range quantifies the distance of autocorrelation caused by the distance between pattern elements. The quality of the fit between the

theoretical and the empirical semivariogram was expressed as RMSE.

Maps were then constructed for a uniform rectangular grid, slightly exceeding the study area by ordinary block kriging (for $5 \times 5\,km^2$ grid cells) using the theoretical semivariogram and all measured data. Sites outside the periphery of the study area were included in the calculation of the map, otherwise the number of samples available for estimations close to the periphery would decrease and be unfavorably distributed in space, both increasing the error variance (Ayyub & McCuen, 1990). The quality of the predictions from the resulting maps was given as the (block) krige standard deviation, which is a measure of the prediction error of an individual block. The krige standard deviations were averaged for the study area. The difference between the P_{C4_SOC} and the P_{C4_VEG} map could then be calculated for each block.

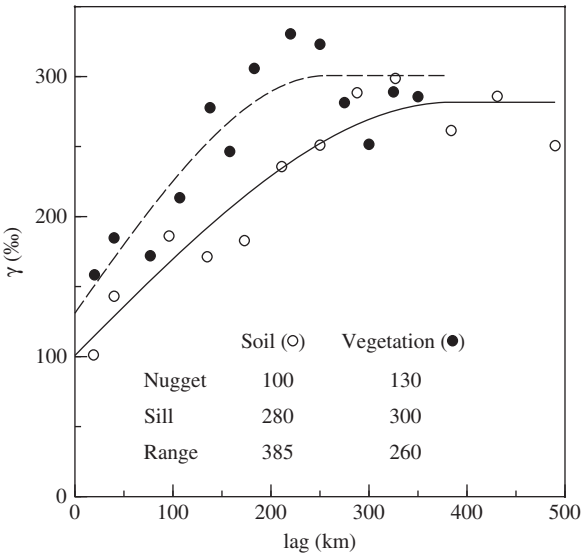

Fig. 3 Empirical (circles) and theoretical (line) semivariograms of percent C4 derived from soil and present (1998–2007) vegetation (the latter semivariogram was taken from Auerswald *et al.*, 2009). RMSEs are 20‰ and 25‰, respectively.

Results

$\delta^{13}C$ of SOC and its relationship to environmental parameters

The $\delta^{13}C_{SOC}$ ranged between −17.4‰ and −26.3‰, with a mean of -22.7 ± 1.8‰ (SD) and a median of −23.0‰ (Fig. 2). The $\delta^{13}C_{SOC}$ responded significantly to mean July temperature (MJulT), MAP, MAT, and altitude (Table 2). All of the correlations were highly significant ($P \ll 0.001$), but altitude explained only 7% of the variation, while the climate parameters explained 30–35%. However, the correlations were not independent, because there were also close correlations between the environmental variables (all $P \ll 0.001$); e.g. MJulT and MAP ($r^2 = 0.88$) or MJulT and altitude ($r^2 = 0.46$). As a result, the effects of environmental variables on $\delta^{13}C_{SOC}$ could not be separated, and each response function of $\delta^{13}C_{SOC}$ to an environmental variable included direct and indirect effects. A multiple regression (MAT, MJulT) explained 37% of the variation, but only the contribution of MJulT was highly significant ($P \ll 0.001$), while that of MAT was only significant ($P < 0.01$).

Geographic variation of C4 abundance

The mean P_{C4_SOC} was 9.7 ± 2.5% (CI) with a median of 7.3% for the study area. The theoretical semivariogram followed a spherical model for P_{C4_SOC} (Fig. 3). The range was approximately 385 km. The nugget effect corresponded to an uncertainty of approximately 14% for P_{C4_SOC} at the sampling locations. The nugget/sill ratio was 0.35 and indicated that 65% of the variation was caused by a spatial pattern. This was far greater than what was explained with regression analysis of $\delta^{13}C_{SOC}$ (Table 2), which assumed (multiple) linear relationships with isolated environmental variables. However, the linear relations of P_{C4_SOC} with altitude, MAP, MAT, and MJulT were narrower than those with $\delta y^{13}{}_{SOC}$. This can be attributed to the removal of the uncertainty at the sampling locations and the short-range noise by kriging $5 \times 5\,km^2$ blocks. MAP, MAT, and MJulT each explained about 40% of the block-average P_{C4_SOC}, while only 10% was explained by altitude (Table 3). A multiple regression (MJulT, MAT) explained 45% of the variation of block averages.

The map of P_{C4_SOC} ranged between 0% and 24% for the individually interpolated $5 \times 5\,km^2$ blocks, with a mean block krige standard deviation of 7% for the study area. The map (Fig. 4a) was characterized by an increase in P_{C4_SOC} from 0% in the southeastern region to around 24% in the western region of the study area near the Gobi desert, and also by a C3-favoring lobe with a P_{C4_SOC} of approximately 1% in the southeast. Collatz *et al.* (1998) obtained an upper limit for the C3/C4 crossover temperature of 20 °C for the warmest month at a volumetric CO_2 concentration of 300 ppm (Table 1). The isotherm of this theoretical crossover temperature essentially separated areas of high and low P_{C4_SOC}. Separated into two areas, MJulT below and above the crossover temperature, P_{C4_SOC} differed very highly significantly (Table 4), by about 15% between the sample sites above the crossover temperature (mean MJulT = 21.6 °C) and the sample sites below (mean

Table 2 Effect of the environmental variables altitude, mean annual precipitation (MAP), mean annual temperature (MAT) and mean July temperature (MJulT) on $\delta^{13}C_{SOC}$ of Inner Mongolia grassland soils quantified by linear regressions; climate means apply for the last normal period 1961–1990, $n = 149$

Parameter	Range	$\delta^{13}C_{SOC}$ response	SE	r^2	P
Altitude	875–1692 m a.s.l.	−2.8‰/1000 m	± 0.001	0.07	$\ll 0.001$
MAP	139–386 mm yr^{-1}	−1.5‰/100 mm yr^{-1}	± 0.002	0.33	$\ll 0.001$
MAT	−0.6–7.5 °C	0.7‰/1 °C	± 0.084	0.31	$\ll 0.001$
MJulT	18.5–23.2 °C	0.7‰/1 °C	± 0.080	0.35	$\ll 0.001$

Table 3 Effect of the environmental variables altitude, mean annual precipitation (MAP), mean annual temperature (MAT) and mean July temperature (MJulT) on kriged P_{C4} of 25 km^2 blocks around the sample sites of Inner Mongolia grassland soils ($n = 149$) quantified by linear regressions; climate means apply for the last normal period 1961–1990

Parameter	Range	Kriged P_{C4} response	SE	r^2	P
Altitude	875–1692 m a.s.l.	−16%/1000 m	± 4	0.10	$\ll 0.001$
MAP	139–386 mm yr^{-1}	−8.4%/100 mm yr^{-1}	± 0.8	0.41	$\ll 0.001$
MAT	−0.6–7.5 °C	3.8%/1 °C yr^{-1}	± 0.4	0.38	$\ll 0.001$
MJulT	18.5–23.2 °C	3.8%/1 °C	± 0.4	0.42	$\ll 0.001$

MJulT = 19.2 °C), despite the flat temperature gradient. This also agreed with the C3 lobe. This extended to the town Abag Qi ('A' in Fig. 4a), which was situated in a small temperature depression ($\sim 70 \times 70$ km^2) where MJulT was below the crossover temperature. This clear separation by the isotherm of the predicted crossover temperature indicated a substantial change within a narrow temperature range, and a spatial dependence on temperature.

Comparison of C4 abundance estimated from SOC with present vegetation

The theoretical semivariogram for P_{C4_VEG} (Auerswald *et al*., 2009) also followed a spherical model (Fig. 3), but had a range that was 125 km less than the range for SOC. The nugget uncertainty was 2% larger than that for SOC, and the nugget/sill ratio indicated that the spatial pattern was less pronounced by approximately 8%. All of the parameters indicated a substantial difference between both patterns. This was confirmed by the maps (Fig. 4), which deviated considerably. P_{C4_VEG} was approximately 10% higher (mean 19.1%) than P_{C4_SOC} (mean 9.7%). This difference was highly significant ($P \ll 0.001$, $\alpha = 0.001$). Again, the structure of the vegetation pattern was related very significantly to the crossover temperature, but only when this was derived for present-day conditions. In contrast, the line of former crossover temperature, which successfully separated high and low P_{C4_SOC}, was a poor predictor for present 10 years average vegetation (Table 4). Analogously, the line of the present crossover temperature poorly separated areas of differing P_{C4_SOC} (Table 4).

The map showing the difference between P_{C4_VEG} and P_{C4_SOC} (Fig. 5) demonstrated that the increase in P_{C4} mainly occurred along an east–west transect from Erenhot ('E' in Fig. 5) to Xilinhot at a latitude of about 44° and in the mountainous area (Da Hinggan Ling mountain ridge) east of Xilinhot ('XH'). Importantly, Fig. 5 was not based on any assumption regarding underlying mechanisms, but it indicated that the latitudinal and altitudinal range of C4 occurrence has expanded. A strong increase took place close to Abag Qi ('A'), where a rather small area previously below the former crossover temperature is now well above the crossover temperature. Almost no change occurred in the north and south of the study area, except for a decrease around Huang Qi ('HQ').

Discussion

Methodological aspects of deriving C3/C4 patterns from SOC

There are two vital and related problems that must be addressed when retrieving P_{C4} from SOC. These are the unknown ^{13}C fractionation during SOC decomposition (Wedin *et al*., 1995), the quantification of soil age, and the resulting isotopic shift between vegetation and SOC caused by the the Suess effect. With increasing soil depth, the soil ages (Rumpel *et al*., 2002; Dümig *et al*., 2008) and the isotopic shift compared with present

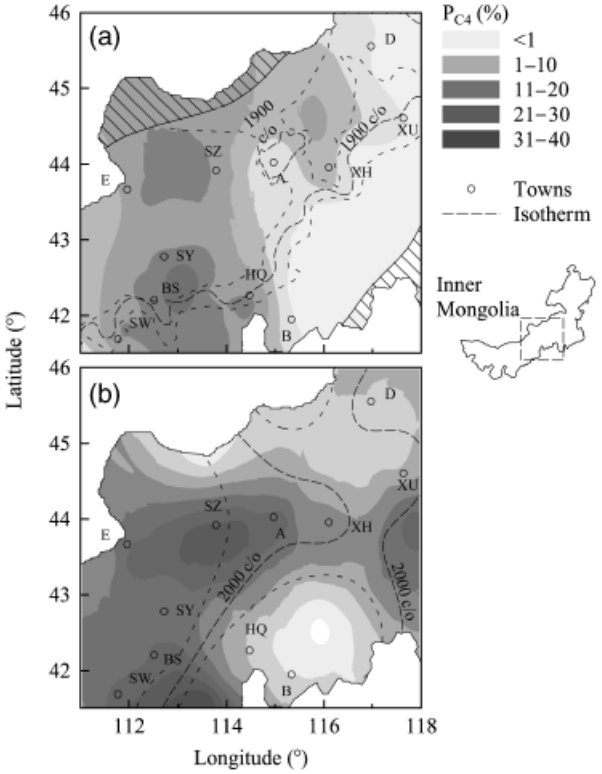

Fig. 4 (a) Regional P_{C4} estimated from SOC; mean krige standard deviation for the study area is 7%. (b) Regional P_{C4} estimated for present vegetation taken from Auerswald *et al.* (2009); mean krige standard deviation for the study area is 9%. Towns are the same as in Fig. 1. The long-dashed lines reflect the isotherms of upper limit for the crossover temperature predicted for the meteorological conditions during the regarded period (1900 vs. 2000), while the short-dashed lines give a range of $\pm$ 0.5 °C around the mean isotherm. Isotherms are not shown for areas were the krige standard deviation exceeded one class (hatched areas, krige SD >10%).

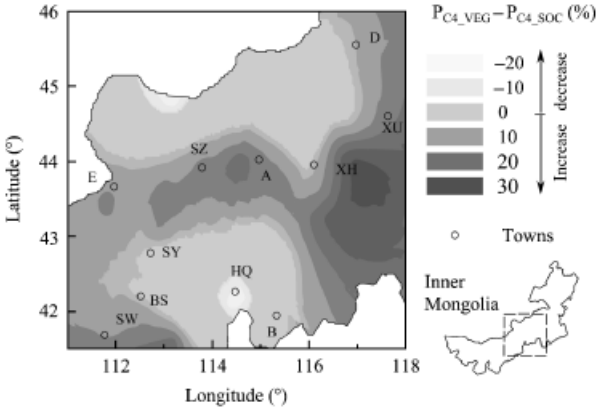

Fig. 5 Difference between P_{C4} of present vegetation (P_{C4_VEG}) and P_{C4} derived from soil (P_{C4_SOC}). Towns are the same as in Fig. 1. To account for uncertainties (absolute) differences smaller than half the maximum krige SD (= 7.5%) were set to zero.

Table 4 Mean contribution of C4 plants (P_{C4}) to vegetation biomass and soil organic carbon for areas of Inner Mongolia separated by the isotherm given by the upper limit of the crossover temperature (c/o) calculated for 1900 and 2000

	P_{C4} below c/o (%)	P_{C4} above c/o (%)	*P*
1900 crossover isotherm			
Soil	1.0	15.9	$\ll 0.001$
Vegetation	14.3	19.1	>0.1
2000 crossover isotherm			
Soil	5.2	11.5	<0.05
Vegetation	10.5	23.3	$\ll 0.001$

P gives statistical probability of identical means within a row.

vegetation increases (e.g. Torn *et al.*, 2002). Following Wynn & Bird's reasoning (2008), we restricted our analysis to the top soil, where both of these influences were smallest and where recent changes in vegetation could be determined. At shallow soil depths, both aboveground and root biomass contribute to SOC, and all of the important species have most of their roots there (Chen *et al.*, 2001) due to the semi-arid climate, in which rainwater during the vegetation period is stored within the first few decimeters of soil.

Apart from the Suess effect, we assumed that no inherent fractionation of $\delta^{13}C_{SOC}$ occurred. Yet we acknowledge that further fractionation-associated uncertainties may exist (von Fischer *et al.*, 2008) and that this may lead to further relative enrichment of $\delta^{13}C_{SOC}$. However, it appears that further fractionations (e.g., due to respiration by invertebrates or microbes) are negligible during early stages of decomposition (Boutton *et al.*, 1998 and citation therein).

The assumed soil age defines the $\delta^{13}C_a$ and the atmospheric CO_2 concentration, and – in turn – influences the crossover temperature. Assuming soil ages >100 years had only a small influence on the crossover temperature; hence, deviating soil ages would bias our calculated crossover temperature only marginally. The influence of atmospheric signature was greater, and substantially changed average P_{C4_SOC} values. In any case, P_{C4_SOC} (6.5%–12.9%, Table 1) was lower than average P_{C4_VEG} (19.1%, Auerswald *et al.*, 2009). While the difference between P_{C4_SOC} and P_{C4_VEG} became smaller with decreasing soil age, P_{C4_VEG} was still higher. With decreasing soil age, the contribution of present vegetation to SOC increased exponentially. Therefore, an even larger contrast with former vegetation would result if decreasing soil age caused a lower P_{C4_SOC} than

in vegetation. For a difference of 6.5% between P_{C4_SOC} and P_{C4_VEG} at a mean SOC age of 50 years, the contrast between mean P_{C4} in vegetation from the last 10 years and the previous 40 years would have to be 8%. As a consequence, the uncertainty caused by the unknown SOC age is not whether P_{C4} has increased, but only whether this increase had occurred more recently and was more rapid (8% within 50 years), or whether the change had occurred over a longer period of time (13% within 300 years).

SOC age should not have an influence on the regional pattern as long as the soil age did not vary spatially. However, there is abundant evidence that SOC turnover is primarily controlled by temperature (references see Wynn & Bird, 2008) e.g. leading to latitudinal gradients in turnover time (Bird *et al*., 2002). The magnitude of the Suess effect observed in the SOC pool should then also increase with MAT or MJulT. In our analysis we applied a regionally constant Suess effect; this should relatively underestimate P_{C4} at higher temperatures. Because the primary observed effect was an increase in P_{C4} with temperature, this increase could not be caused by regionally varying decomposition rates, but may be even somewhat larger than our estimate.

Land use change and the spatiotemporal variation in C3/C4 composition

Three drivers are likely to cause changes in P_{C4}; namely, land-use change, change in CO_2 concentration, and temperature change. Land use was mainly influenced by the transition from nomadic to sedentary life style in the 1960s (Humphrey & Sneath, 1995), and by the fast economic rise in the 1990s (e.g. Xu & Zhang, 2007). Although these drivers were active within the entire study area, their effect may have differed between herders, because of differences in attitude and access to markets. Hence, land use changes would most likely result in small-scale changes, which should increase the nugget effect and decrease the range in the semivariogram (Rossi *et al*., 1992). Both of these modifications were observed. The nugget effect of present vegetation was larger than that of soil, despite the method of retrieving the vegetation pattern from wool, which eliminated the small-scale variation within the grazing ground of a flock of sheep, and thus lowered the nugget effect. Given the patchiness of the vegetation, the nugget effect would have been much larger if the vegetation had been sampled on the same spatial scale ($20 \times 20\,cm^2$) as the soil, because of the decreasing so-called 'support' (i.e. the spatial extent for which the measured value for the property is valid) increasing the nugget effect (Webster, 1991). Sampling wool, however, conserved the variation between vicinal herds, thus contributing to the nugget effect. Further, the decrease in the range of the present vegetation compared with soil supported land use as a main driver. However, the pronounced regional pattern in the change of P_{C4} (Fig. 5) was likely not related to these land use changes.

CO_2 concentration change and the spatiotemporal variation in C3/C4 composition

Changes in CO_2 concentration should have decreased P_{C4} in the entire area, thus reducing the competitiveness of C4 plants (Ehleringer *et al*., 1997). The present data contrast with this prediction. P_{C4} increased, and this occurred in a pronounced pattern. Moreover, this increase was independent of P_{C4_SOC} (Table 1). Very clearly, the increase in CO_2 concentration was unlikely to have caused the change in the P_{C4} pattern. Yet, it may have attenuated the increase in P_{C4}, and it may explain why, in the southwestern part of the study area, P_{C4} actually decreased.

Temperature change and the spatiotemporal variation in C3/C4 composition

Changes in temperature should also cause large-scale changes, but because temperature change varies regionally, this effect was perhaps not homogenous within the area. The regional variation in temperature change became obvious when comparing the line of the present crossover temperature on the vegetation map with the line of the former crossover temperature on the soil map (Fig. 4). Although the present crossover temperature is expected to be 2 °C higher due to the increase in CO_2 concentration, both isotherms should still be near parallel if the temperature pattern has not changed. However, this was not the case. While the former crossover temperature isotherm essentially extended SW–NE, the present crossover temperature extended SSW–NNE and crossed the former one, indicating a substantial change in the temperature pattern. Both P_{C4} patterns basically followed the predicted crossover temperatures of the respective periods. The 'true' crossover temperature may have differed because species/metabolic groups may differ in quantum yield (Ehleringer *et al*., 1997). Moreover, MJulT is only a proxy for leaf temperature (Teeri, 1988; Wynn & Bird, 2008), which is the direct control of photosynthesis in C3 and C4 plants (Ehleringer & Björkman, 1977). Also, the true crossover temperature for SOC may deviate from that calculated for the last normal period (1961–1990) depending on the temporal integration of SOC. This potential bias should be small as no distinct warm or cold period occurred between 1700 and 1970 (Liu *et al*., 2009) and most of the

SOC was formed after 1960. E.g. approximately 40% of total SOC was formed after 1960 assuming a SOC age of 100 years [Eqn (2)]. Hence, it can still be expected that the true lines were near parallels of the most likely crossover temperatures, as shown in Fig. 4, and thus would also explain the pattern.

The effect of even a constant temperature increase would differ depending on the initial conditions. A temperature increase should be most effective in areas close to the crossover temperature, while it becomes marginal at temperatures well above or below. The largest increase in P_{C4} (Fig. 5) occurred within a latitudinal belt along 44°N and in the only mountainous area in the east, indicating that the increase in temperature has enlarged the latitudinal and altitudinal range in which C4 successfully competed with C3. This is in agreement with a recent finding by von Fischer *et al*. (2008) showing that the competition between C3 and C4 in North American grasslands was particularly sensitive to changes in summer temperature.

Hence, temperature changes appeared to be the main driver for the change in P_{C4}, while the change in CO_2 concentration likely attenuated this effect. Land use changes may have added local variation. The interaction of many drivers in creating the pattern was also evident from the poor performance of the linear and multiple regressions in explaining the variation despite the pronounced pattern that was evident from the nugget/sill ratio and the maps. Geostatistical analysis does not depend upon predefined variables and types of relation, e.g. linear, polynomic or exponential. Instead, it quantifies the autocorrelation depending on distance, revealing the response of vegetation in a complex web of interactions. This is necessary because estimates of the terrestrial ^{13}C discrimination must take into account ecophysiological processes on the leaf and plant scale, translate these processes into regional or global scales (Lloyd & Farquhar, 1994; Still *et al*., 2003; Wynn & Bird, 2008), and enable quantification of the change and range of underlying patterns.

Conclusions

This work indicates that P_{C4} of Inner Mongolia grassland has increased by approximately 10% in the past decades. Although there are uncertainties regarding inherent fractionation during SOC formation, turnover and age, these appear to be much smaller than the change revealed by the isotope data. In particular, these uncertainties would not account for the distinct relationships of these changes with weather factors. The main driver for the increased P_{C4} appeared to be regional warming, which increased the latitudinal and altitudinal range of C4 plants. Both patterns of P_{C4}, in recent vegetation and in SOC, followed the predictions derived from crossover temperature of quantum yield for CO_2 fixation in modern time and in the period of SOC formation.

Acknowledgements

This research was funded by the DFG within the DFG research group 536 (MAGIM) and the Natural Science Foundation of China (30825008, 30770370). We thank Martin Wiesmeier (Technische Universität München, Lehrstuhl für Bodenkunde) and Yang Hao for assistance during sampling and Monika Michler for assistance with sample preparation for isotopic analysis.

References

Allison CE, Francey RJ, Krummel PB (2003) $\delta^{13}C$ in CO_2 from sites in the CSIRO Atmospheric Research GASLAB air sampling network (April 2003 version). In: *Trends: A Compendium of Data on Global Change*. Carbon Dioxide Information Analysis Center, Oak Ridge National Laboratory, U.S. Department of Energy, Oak Ridge, TN, USA. Available at http://cdiac.ornl.gov/trends/co2/allison-csiro/allcsiro-shetland.html (accessed 10 October 2008).

Auerswald K, Wittmer MHOM, Männel TT, Bai YF, Schäufele R, Schnyder H (2009) Large regional-scale variation in C3/C4 distribution pattern in Inner Mongolia steppe is revealed by grazer wool carbon isotope composition. *Biogeosciences*, **6**, 795–805.

Ayyub BM, McCuen RH (1990) Optimum sampling for structural strength evaluation. *Journal of Structural Engineering*, **116**, 518–535.

Bachmaier M, Backes M (2008) Variogram or semivariogram? Understanding the variances in a variogram. *Precision Agriculture*, **9**, 173–175.

Bird MI, Pousai P (1997) Variations of $\delta^{13}C$ in the surface soil organic carbon pool. *Global Biogeochemical Cycles*, **11**, 313–322.

Bird MI, Santruckova H, Arneth H *et al*. (2002) Soil carbon inventories and carbon-13 on a latitudinal transect in Siberia. *Tellus*, **54B**, 631–641.

Boutton TW, Archer SR, Midwood AJ, Zitzer SF, Bol R (1998) $\delta^{13}C$ values of soil organic carbon and their use in documenting vegetation change in a subtropical savanna ecosystem. *Geoderma*, **82**, 5–41.

Chen S, Zhang H, Wang L, Hai B, Zhao M (2001) *Roots of Grassland Plants in Northern China*. Jilin University Press, Changchun.

Collatz GJ, Berry JA, Clark JS (1998) Effects of climate and atmospheric CO_2 partial pressure on the global distribution of C4 grasses: present, past, and future. *Oecologia*, **114**, 441–454.

Conway TJ, Tans PP, Waterman LS (1994) Atmospheric CO_2 records from sites in the NOAA/CMDL air sampling network. In: *Trends '93: A Compendium of Data on Global Change*. Carbon Dioxide Information Analysis Center, Oak Ridge National Laboratory, US Department of Energy, Oak Ridge, TN, USA.

Daly C, Gibson WP, Taylor GH, Johnson GL, Pasteris P (2002) A knowledge-based approach to the statistical mapping of climate. *Climate Research*, **22**, 99–113.

Dümig A, Schad P, Rumpel C, Dignac MF, Kögel-Knabner I (2008) Araucaria forest expansion on grassland in the southern Brazilian highlands as revealed by 14C and $\delta^{13}C$ studies. *Geoderma*, **145**, 143–157.

Ehleringer JR, Björkman O (1977) Quantum yields for CO_2 uptake in C3 and C4 plants – dependence on temperature, CO_2, and O_2 concentration. *Plant Physiology*, **59**, 86–90.

Ehleringer JR, Buchmann N, Flanagan LB (2000) Carbon isotope ratios in belowground carbon cycle processes. *Ecological Applications*, **10**, 412–422.

Ehleringer JR, Cerling TE, Helliker BR (1997) C4 photosynthesis, atmospheric CO_2 and climate. *Oecologia*, **112**, 285–299.

Epstein HE, Burke IC, Mosier AR (1998) Plant effects on spatial and temporal patterns of nitrogen cycling in shortgrass steppe. *Ecosystems*, **1**, 374–385.

Farquhar GD, Ehleringer JR, Hubick KT (1989) Carbon isotope discrimination and photosynthesis. *Annual Review of Plant Physiology and Plant Molecular Biology*, **40**, 503–537.

Francey RJ, Allison CE, Etheridge DM *et al*. (1999) A 1000-year high precision record of δ^{13}C in atmospheric CO_2. *Tellus*, **51B**, 170–193.

Friedli H, Lötscher H, Oeschger H, Siegenthaler U, Stauffer B (1986) Ice core record of the $^{13}C/^{12}C$ ratio of atmospheric CO_2 in the past two centuries. *Nature*, **324**, 237–238.

Gao Q, Yu M, Yang XS (2000) An analysis of sensitivity of terrestrial ecosystems in China to climatic change using spatial simulation. *Climatic Change*, **47**, 373–400.

Gat JR, Mook WG, Meijer HAJ (2001) *Environmental isotopes in the hydrological cycle, principles and applications*. Vol. II, Atmospheric water, Available at http://www-naweb.iaea.org/napc/ih/IHS_resources3_publication_en.html (accessed 10 October 2008).

Harris D, Horwath WR, van Kessel C (2001) Acid fumigation of soils to remove carbonates prior to total organic carbon or ^{13}C isotopic analysis. *Soil Science Society of America Journal*, **65**, 1853–1856.

Hattersley PW (1983) The distribution of C3 and C4 grasses in Australia in relation to climate. *Oecologia*, **57**, 113–128.

Humphrey C, Sneath D (1995) Pastoralism and institutional change in Inner Asia: comparative perspectives from the MECCIA research project. *Pastoral Development Network Series*, **39**, 2–23.

Keeling CD, Mook WG, Tans PP (1979) Recent trends in the C-13–C-12 ratio of atmospheric carbon-dioxide. *Nature*, **277**, 121–123.

Krull ES, Bray S, Harms B, Baxter N, Bol R, Farquhar G (2007) Development of a stable isotope index to assess decadal-scale vegetation change and application to woodlands of the Burdekin catchment, Australia. *Global Change Biology*, **13**, 1455–1468.

Krull ES, Skjemstad JO, Burrows WH *et al*. (2005) Recent vegetation change in central Queensland, Australia: evidence from δ^{13}C and ^{14}C analyses of soil organic matter. *Geoderma*, **126**, 241–259.

Li J, Zhou MZ, Du GH *et al*. (1978) *Soils Map of China (1:4,000,000)*. Academia Sinica Science Press, Beijing.

Liu WG, Feng XH, Ning YF, Zhang QL, Cao YN, An ZS (2005) δ^{13}C variation of C3 and C4 plants across an Asian monsoon rainfall gradient in arid northwestern China. *Global Change Biology*, **11**, 1094–1100.

Liu Y, An ZS, Linderholm HW *et al*. (2009) Annual temperatures during the last 2485 years in the mid-eastern Tibetan Plateau inferred from tree rings. *Science in China D: Earth Sciences*, **52**, 348–359.

Lloyd J, Farquhar GD (1994) ^{13}C discrimination during CO_2 assimilation by the terrestrial biosphere. *Oecologia*, **99**, 201–215.

Lopez-Capel E, Krull ES, Bol R, Manning DAC (2008) Influence of recent vegetation on labile and recalcitrant carbon soil pools in central Queensland, Australia: evidence from thermal analysis-quadrupole mass spectrometry-isotope ratio mass spectrometry. *Rapid Communications in Mass Spectrometry*, **22**, 1751–1758.

Männel TT, Auerswald K, Schnyder H (2007) Altitudinal gradients of grassland carbon and nitrogen isotope composition are recorded in the hair of grazers. *Global Ecology and Biogeography*, **16**, 583–592.

Ni J (2003) Plant functional types and climate along a precipitation gradient in temperate grasslands, north-east China and south-east Mongolia. *Journal of Arid Environments*, **53**, 501–516.

NOAA ESRL (2008) *Earth System Research Laboratory*. Global Monitoring Division. Available at http://www.esrl.noaa.gov/gmd (accessed 10 October 2008).

NOAA NCDC Climate Data Online (2008). Available at http://cdo.ncdc.noaa.gov/CDO/cdo (accessed 4 September 2008).

Paruelo JM, Lauenroth WK (1996) Relative abundance of plant functional types in grasslands and shrublands of North America. *Ecological Applications*, **6**, 1212–1224.

Pebesma EJ (2004) Multivariable geostatistics in S: the gstat package. *Computers & Geosciences*, **30**, 683–691.

Pyankov VI, Gunin PD, Tsoog S, Black CC (2000) C4 plants in the vegetation of Mongolia: their natural occurrence and geographical distribution in relation to climate. *Oecologia*, **123**, 15–31.

R Development Core Team (2008) *R: A language and environment for statistical computing, R Foundation for Statistical Computing*. ISBN 3-900051-07-0. Available at http://www.R-project.org, Vienna, Austria.

Ribeiro PJ, Diggle PJ (2001) geoR: a package for geostatistical analysis. *R-NEWS*, **1**, 15–18.

Rossi RE, Mulla DJ, Journel AG, Franz EH (1992) Geostatistical tools for modeling and interpreting ecological spatial dependence. *Ecological Monographs*, **62**, 277–314.

Rumpel C, Kögel-Knabner I, Bruhn F (2002) Vertical distribution, age and chemical composition of organic carbon in two forest soils of different pedogenesis. *Organic Geochemistry*, **33**, 1131–1142.

Sachs L, Hedderich J (2006) *Angewandte Statistik. Methodensammlung mit R*. Springer, Berlin.

Sage RF, Kubien DS (2003) Quo vadis C4? An ecophysiological perspective on global change and the future of C4 plants. *Photosynthesis Research*, **77**, 209–225.

Santruckova H, Bird MI, Lloyd J (2000) Microbial processes and carbon-isotope fractionation in tropical and temperate grassland soils. *Functional Ecology*, **14**, 108–114.

Schimel DS (1995) Terrestrial ecosystems and the carbon-cycle. *Global Change Biology*, **1**, 77–91.

Schnute JT, Boers N, Haigh R, Couture-Beil A (2008) PBSmapping: PBS Mapping 2.59, R package version 2.59.

Semmartin M, Aguiar MR, Distel RA, Moretto AS, Ghersa CM (2004) Litter quality and nutrient cycling affected by grazing-induced species replacements along a precipitation gradient. *Oikos*, **107**, 148–160.

Silvermann BW (1986) Density estimations for statistics and data analysis. In: *Monographs on Statistics and Applied Probability*, Vol. 26 (eds Cox DR, Hinkley DV, Reid N, Rubin DB, Silvermann BW) Chapman & Hall/CRC, London, UK.

Still CJ, Berry JA, Collatz GJ, DeFries RS (2003) Global distribution of C3 and C4 vegetation: carbon cycle implications. *Global Biogeochemical Cycles*, **17**, 1006.

Tans PP, Conway TJ (2005) Monthly atmospheric CO2 mixing ratios from the NOAA CMDL Carbon Cycle Cooperative Global Air Sampling Network, 1968–2002. In: *A Compendium of Data on Global Change*. Carbon Dioxide Information Analysis Center, Oak Ridge National Laboratory, US Department of Energy, Oak Ridge, TN, USA. Available at http://cdiac.esd.ornl.gov/trends/co2/cmdl-flask/cmdl-flask.html (accessed 10 October 2008).

Teeri JA (1988) Interaction of temperature and other environmental variables influencing plant distribution. *Symposia of the Society for Experimental Biology*, **42**, 77–89.

The Climate Source LLC, Corvallis, OR, USA (2002) PRISM spatial climate datasets for Mongolia and Inner Mongolia.

Tieszen LL, Reed BC, Bliss NB, Wylie BK, Dejong DD (1997) NDVI, C3 and C4 production, and distributions in great plains grassland land cover classes. *Ecological Applications*, **7**, 59–78.

Torn MS, Lapenis AG, Timofeev A, Fischer ML, Babikov BV, Harden JW (2002) Organic carbon and carbon isotopes in modern and 100-year-old-soil archives of the Russian steppe. *Global Change Biology*, **8**, 941–953.

Trumbore S (2000) Age of soil organic matter and soil respiration: radiocarbon constraints on belowground C dynamics. *Ecological Applications*, **10**, 399–411.

von Fischer JC, Tieszen LL, Schimel DS (2008) Climate controls on C3 vs. C4 productivity in North American grasslands from carbon isotope composition of soil organic matter. *Global Change Biology*, **14**, 1141–1155.

Wang RZ (2002) Photosynthetic pathways, life forms, and reproductive types for forage species along the desertification gradient on Hunshandake desert, North China. *Photosynthetica*, **40**, 321–329.

Wang RZ (2003) Photosynthetic pathway and morphological functional types in the steppe vegetation from Inner Mongolia, North China. *Photosynthetica*, **41**, 143–150.

Wang RZ (2004) Photosynthetic and morphological functional types from different steppe communities in Inner Mongolia, North China. *Photosynthetica*, **42**, 493–503.

Webster R (1991) Local disjunctive kriging of soil properties with change of support. *Journal of Soil Science*, **42**, 301–318.

Wedin DS, Tieszen LL, Dewey B, Pastor J (1995) Carbon isotope dynamics during grass decomposition and soil organic matter formation. *Ecology*, **76**, 1383–1392.

Wittmer MHOM, Auerswald K, Tungalag R, Bai YF, Schäufele R, Schnyder H (2008) Carbon isotope discrimination of C3 vegetation in Central Asian Grassland as related to long-term and short-term precipitation patterns. *Biogeosciences*, **5**, 913–924.

Wynn JG, Bird MI (2007) C4-derived soil organic carbon decomposes faster than its C3 counterpart in mixed C3/C4 soils. *Global Change Biology*, **13**, 2206–2217.

Wynn JG, Bird MI (2008) Environmental controls on the stable carbon isotopic composition of soil organic carbon: implications for modeling the distribution of C3 and C4 plants, Australia. *Tellus*, **60B**, 604–621.

Xiao X, Ojima DS, Parton WJ, Chen Z, Chen D (1995) Sensitivity of Inner Mongolia grasslands to climate change. *Journal of Biogeography*, **22**, 643–648.

Xu M, Zhang TZ (2007) Material flows and economic growth in developing China. *Journal of Industrial Ecology*, **11**, 121–140.

Yu FF, Price KP, Ellis J, Shi PJ (2003) Response of seasonal vegetation development to climatic variations in eastern central Asia. *Remote Sensing of Environment*, **87**, 42–54.

Zhao FJ, Spiro B, McGarth SP (2001) Trends in $^{13}C/^{12}C$ ratios and isotope discrimination of wheat since 1845. *Oecologia*, **128**, 336–342.

Supporting Information

Additional Supporting Information may be found in the online version of this article:

Table S1. Coefficients for the cubic polynomial models for the prediction of $\delta^{13}C_a$; the independent variable is the year/1000.

Figure S1. Atmospheric carbon isotope composition ($\delta^{13}C_a$, circles, solid line) and atmospheric CO_2 concentration (dashed line) (Keeling, 1979; Friedli *et al*., 1986; Conway *et al*., 1994; Francey *et al*., 1999; Gat *et al*., 2001; Allison *et al*., 2003; NOAA ESRL, 2008). Grey and white areas denote different fitting models (Table S1).

Please note: Wiley-Blackwell are not responsible for the content or functionality of any supporting materials supplied by the authors. Any queries (other than missing material) should be directed to the corresponding author for the article.